Stem Cell Reviews and Reports (2021) 17:459–470
https://doi.org/10.1007/s12015-020-10078-7

Protective Effects of Human Liver Stem Cell-Derived Extracellular Vesicles in a Mouse Model of Hepatic Ischemia-Reperfusion Injury

Alberto Calleri[1] · Dorotea Roggio[1] · Victor Navarro-Tableros[2] · Nicola De Stefano[1] · Chiara Pasquino[3] · Ezio David[4] · Giada Frigatti[1] · Federica Rigo[1] · Federica Antico[5] · Paola Caropreso[6] · Damiano Patrono[1] · Stefania Bruno[3] · Renato Romagnoli[1]

Accepted: 31 October 2020 / Published online: 2 December 2020

Abstract

Hepatic ischemia-reperfusion injury (IRI) is observed in liver transplantation and hepato-biliary surgery and is associated with an inflammatory response. Human liver stem cell-derived extracellular vesicles (HLSC-EV) have been demonstrated to reduce liver damage in different experimental settings by accelerating regeneration and by modulating inflammation. The aim of the present study was to investigate whether HLSC-EV may protect liver from IRI in a mouse experimental model. Segmental IRI was obtained by selective clamping of intrahepatic pedicles for 90 min followed by 6 h of reperfusion. HLSC-EV were administered intravenously at the end of the ischemic period and histopathological and biochemical alterations were evaluated in comparison with controls injected with vehicle alone. Intra liver localization of labeled HLSC-EV was assessed by in in vivo Imaging System (IVIS) and the internalization into hepatocytes was confirmed by fluorescence analyses. As compared to the control group, administration of 3×10^9 particles (EV1 group) significantly reduced alanine aminotransferase (ALT) and lactate dehydrogenase (LDH) release, necrosis extension and cytokines expression (TNF-α, CCL-2 and CXCL-10). However, the administration of an increased dose of HLSC-EV (7.5×10^9 particles, EV2 group) showed no significant improvement in respect to controls at enzyme and histology levels, despite a significantly lower cytokine expression. In conclusion, this study demonstrated that 3×10^9 HLSC-EV were able to modulate hepatic IRI by preserving tissue integrity and by reducing transaminases release and inflammatory cytokines expression. By contrast, a higher dose was ineffective suggesting a restricted window of biological activity.

Keywords Ischemia-reperfusion · Hepatic inflammation · Adult stem cells · Microvesicles · Liver regeneration

This article belongs to the Topical Collection: *Special Issue on Exosomes and Microvesicles: from Stem Cell Biology to Translation in Human Diseases*
Guest Editor: Giovanni Camussi

✉ Renato Romagnoli
renato.romagnoli@unito.it

Alberto Calleri
alberto.calleri.md@gmail.com

Dorotea Roggio
dorotea.roggio@unito.it

Victor Navarro-Tableros
victor.navarro@2i3t.it

Nicola De Stefano
destefano.nicola@libero.it

Chiara Pasquino
chiara.pasquino@unito.it

Ezio David
ezio.david@unito.it

Giada Frigatti
giada.frigatti@edu.unito.it

Federica Rigo
federica.rigo@unito.it

Federica Antico
federica.antico@unito.it

Paola Caropreso
pcaropreso@cittadellasalute.to.it

Damiano Patrono
damiano.patrono@unito.it

Stefania Bruno
stefania.bruno@unito.i

Extended author information available on the last page of the article

Introduction

Hepatic ischemia-reperfusion injury (IRI) is an antigen-independent inflammatory response commonly observed when blood supply is restored after surgical procedures such as liver resection and transplantation. This phenomenon is initiated in Kupffer cells and hepatocytes by a burst in reactive oxygen species (ROS) production in mitochondria after organ reperfusion [1]. ROS production leads to hepatocyte and endothelial cell damage, promoting the recruitment of neutrophils and T-cells and starting an inflammatory cascade that eventually triggers apoptosis and necrosis [2–4]. In liver transplantation, IRI can cause early graft failure or dysfunction, and it is associated with a higher incidence of acute and chronic rejection [5].

Adult human liver stem-like cells (HLSC) were identified as a population of pluripotent resident liver cells expressing both markers characteristic of the mesenchymal lineage (CD29, CD44, CD73, CD90, CD105) and hepatic markers (albumin and alpha-fetoprotein), suggesting a partial hepatic commitment. [6] Moreover, these cells express vimentin, nestin, Musashi stem cell markers and nanog, SSEA4, pax2, and octa4 embryonic stem cell markers. [7, 8] HLSC were shown to localize within the injured tissue and to promote liver regeneration in a murine model of fulminant liver failure [7] and to increase kidney recovery in a murine model of acute kidney injury [8]. When seeded in acellular liver scaffold, HLSC were shown to differentiate into mature functional hepatocytes [9]. More recently, a phase 1 study demonstrated the safety of HLSC administration in infants with neonatal hyperammonemia [10]. Growing evidence supports the hypothesis that the biological effects of stem cells on neighboring cells are mediated by paracrine mechanisms related to the release of soluble factors and extracellular vesicles (EV) [11, 12]. EV are a heterogeneous population of cell-derived membrane vesicles originating from the endosomal compartment or from direct budding of plasma membrane, which are able to modulate phenotype and function of neighboring cells [13–15]. Several studies suggest that EV contribute to the regenerative effect of stem cells through a horizontal transfer of biological active proteins, lipids and specific subsets of messenger RNA and microRNA (miRNA) [16–19]. In particular, we demonstrated that EV derived from HLSC (HLSC-EV) were able to reduce apoptosis and to promote hepatocyte proliferation in a mouse model of partial hepatectomy [20]. More recently, we described the biological effects of HLSC-EV on livers perfused ex-vivo under hypoxic conditions [21]. Moreover, a protective role of HLSC-EV was demonstrated in a murine model of diet-induced non-alcoholic steatohepatitis (NASH) by showing anti-fibrotic and anti-inflammatory effects [19].

The regenerative properties of HLSC-EV have not been so far tested in a model of warm hepatic IRI. In liver resection, intermittent clamping of the hepatic pedicle (Pringle maneuver) is frequently employed to reduce blood loss during parenchymal transection, exposing liver cells to warm IRI and favoring post-hepatectomy liver failure. The latter is one of the main concerns after liver resection and a major determinant of postoperative morbidity and mortality.

The aim of the present study was to investigate whether HLSC-EV have a potential application in the setting of liver surgery by evaluating their effect in an experimental mouse model of warm hepatic IRI.

Materials and Methods

Animals

Animal studies were performed following a protocol approved by the Ethic Committee of the Italian Institute of Health (Istituto Superiore di Sanità, N.62/2016-PR). Male C57BL/6 mice at 8–10 weeks of age were used in all experiments and were housed in Molecular Biotechnology Center (Turin, Italy) animal facility under specific pathogen-free conditions, receiving human care according to the criteria of the National Institute of Health Guide for Care and Use of Laboratory Animals. Mice were maintained on a 12-h dark–light cycle and allowed free access to standard food and water. All experiments were conducted during the light cycle.

Mouse Model of Liver IRI

Total anesthesia was induced through an intramuscular injection of tiletamine-zolazepam (Zoletil®) (0.2 mg/Kg) and xilazine (Rompun®) (16 mg/Kg). After a midline laparotomy, the falciform ligament was cut and the liver mobilized, allowing the exposure of the hepatic hilum. Vascular pedicles to the left lateral and median lobes (approximately 70% of total liver parenchyma) were clamped using an atraumatic clamp for 90 min. The non-ischemic lobes guaranteed a portocaval shunt avoiding intestinal congestion during the ischemic period (supplementary material 1). To prevent hypothermia, the abdomen was closed with a cutaneous running suture (silk 6/0) and the animal was kept warm under an infrared lamp. After 90 min of warm ischemia, the laparotomy was reopened and the clamp removed, allowing reperfusion of the whole liver. Immediately after reperfusion, HLSC-EV or vehicle (saline), according to the experimental group, were administered through the tail vein.

A total of 40 mice were used in the study. Animals were randomly shuffle ordered within four groups. From them, two mice were excluded from the analysis because one died by complications during anesthesia, while the second one was excluded because less than 70% of the liver parenchyma showed to be ischemic. Thereby, 38 mice, comparable in size and weight, were included in the analysis, and the groups were defined as follows: a) EV1 group ($n = 10$) received 3×10^9

HLSC-EV diluted in 120 μl of saline; b) EV2 group ($n = 9$) received 7.5×10^9 HLSC-EV diluted in 120 μl of saline; c) control group (n = 10) received 120 μl of saline; and d) sham operated group (n = 9).

All the animals from control, EV1 and EV2 groups underwent the laparotomy and clamping surgical procedures, followed by the intravenous injection (saline or HLSC-EV), while the sham group underwent the same surgical procedure except for the clamping and the intravenous injection.

All surgeries and intravenous injections were performed by the same operator. After being anesthetized, all the animals were sacrificed after 6 h post-reperfusion by exsanguination and cervical dislocation, then tissue samples were collected.

All the analyses included in our study (IVIS, biochemistry, histology and molecular biology) were blindly performed by different investigators.

Isolation, Characterization and Culture of HLSC

The HLSC were isolated from human cryopreserved hepatocytes obtained from Lonza, Bioscience (Basel, Switzerland) as previously described [8]. The HLSC were cultured in a medium containing a 3:1 proportion of α-minimum essential medium and endothelial cell basal medium-1, supplemented with L-glutamine 2 mM, penicillin 100 U/mL, streptomycin 100 μg/mL and 10% fetal calf serum (α-MEM/EBM/FCS), and maintained in a humidified 5% CO_2 incubator at 37°C [6]. HLSC at passages 5 to 8 were used in all the experiments.

HLSC were positive for CD73, CD90, CD105, CD29 and CD44 and negative for CD45, CD14, CD34, CD117 (c-kit) and CD133.

Isolation and Characterization of HLSC-EV

The HLSC-EV were obtained as previously described [20]. Briefly, the HLSC were starved overnight in RPMI medium deprived of FCS at 37°C in a humidified incubator with 5% CO_2. Viability of cells evaluated by trypan blue exclusion at the time of supernatant collection was >95%. Supernatants were collected, centrifuged for 30 min at 3000 g and submitted to microfiltration with 0.22-mm filters to remove cell debris and apoptotic bodies. Supernatants were then collected and ultracentrifuged at 100,000 g for 2 h at 4°C (Beckman Coulter Optima L-90 K, Fullerton, CA, USA). EV were collected and labelled with 1 μM of Dil dye and 1 μM of Did dye (1,1′-dioctadecyl-3,3,3′,3′- tetramethylindocarbocyanine perchlorate, Dil; 1,1′-dioctadecyl- 3,3,3′,3′-tetramethylindodicarbocyanine, 4-chlorobenzenesulfonate, Did; both from Molecular Probes Life Technology, New York, NY, USA), then washed in phosphate buffered saline (PBS) and ultracentrifugated for 1 h at 4°C [22]. The collected Dil-Did stained EV were used fresh or stored at −80°C after re-suspension in RPMI and 1% dimethyl sulfoxide. No differences in biological activity were observed between fresh and stored EV (data not shown). Quantification and size distribution of EV diluted (1:200) in sterile saline solution were performed by using NanoSight LM10 (NanoSight Ltd., Minton Park, UK) with the NTA 1.4 Analytical Software as previously described [23].

HLSC-EV were characterized by bead-based multiplex analysis by flow cytometry (MACSPlex Exosome Kit, human, Miltenyi Biotec) [24, 25]. Briefly, 1×10^9 EV were diluted with MACSPlex buffer (MPB) to a final volume of 120 μL and loaded into a 1.5-mL tube. Thereafter, 15 μL MACSPlex Exosome Capture Beads (containing 39 different antibody-coated bead subsets) was added to each tube. To stain EV bound to beads, 5 μL of APC-conjugated anti-CD9, anti-CD63, and anti-CD81 detection antibodies were added to each tube and then incubated in an orbital shaker for 1 h at 450 rpm at room temperature in the dark. Beads were washed with 1 mL MPB and centrifuged at 3000 g for 5 min. A second step of washing with 1 mL MPB was performed by incubation in an orbital shaker at 450 rpm, in the dark for 15 min at room temperature and then submitted to centrifugation at 3000 g for 5 min. Flow-cytometric analysis was performed with a CytoFLEX instrument (Beckman Coulter, Brea, CA, USA) recording approximately 5000–8000 single-bead events per sample.

After background correction, the median fluorescence intensity (MFI) of all 39-capture beads subsets was recorded. All bead populations can be identified and gated based on their respective fluorescence intensity according to the manufacturer's instructions.

For transmission electron microscopy analysis EV were placed on 200-mesh nickel formvar carbon-coated grids (Electron Microscopy Science, Hatfield, PA, USA) and after 20 min adhesion, followed by washing in PBS, EV were fixed with 2.5% glutaraldehyde containing 2% sucrose. After repeated washings in distilled water, the EV were negatively stained with NanoVan (Nanoprobes, Yaphank, NY, USA) and observed using a Jeol JEM 1010 electron microscope (Jeol, Tokyo, Japan) as previously described [26].

Hepatocellular Function

Blood samples were collected by cardiac puncture; serum was then separated by centrifugation (10 min at 1200 g) and stored at −80°C. Serum levels of aspartate amino-transferase (AST), alanine amino-transferase (ALT) and lactate dehydrogenase (LDH) were assessed by standard absorption techniques at the biochemistry laboratory (Baldi e Riberi – Molinette Hospital).

IVIS Analysis

Biodistribution analyses were performed using IVIS 200 small animal imaging system (Perkin Elmer, Waltham, MA, USA). After six hours, mice were sacrificed and organs

collected. Hence, liver, kidneys, heart, lungs, spleen, pancreas were placed in a non-fluorescent Petri dish and the filters were set at 640 nm (Ex) and 700 nm (Em). Images were acquired and analyzed using Living Image 4.0 software (Perkin Elmer) through the designation of regions-of-interest. The fluorescence intensity was obtained and expressed as the Average Radiant Efficiency ([p/s/cm^2/sr] / [μW/cm^2]).

Histological Analysis

Tissue biopsies collected from the ischemic lobes were formalin fixed and paraffin embedded for hematoxylin-eosin staining (H&E). The severity of histological damage was blindly scored by an experienced liver pathologist (E.D.) using the Suzuki's Score: according to this system, congestion, ballooning degeneration and necrosis are graded from 0 to 4 [27].

HLSC-EV uptake was analyzed by immunofluorescence microscopy. After rinsing in PBS, slices were incubated for 5 min at 4°C with a permeabilization solution containing 20 mmol/l Hepes, 50 mmol/L NaCL, 300 mmol/L sucrose, 3 mmol/L MagCl2, 0,5% Triton X- 100, pH 7.4. After washing with PBS, slices were incubated for 1 h at room temperature with a blocking solution of PBS added with 3% bovine albumin (both from Sigma-Aldrich) and incubated overnight at 4°C with an anti-mouse cytokeratin-8 primary antibody (1:200) (Abcam). At the end of the incubation, they were washed with PBS and then incubated for 1 h at room temperature with the Alexa Fluor 488-conjugated secondary antibody (1:200) (Invitrogen). Thereby, slices were washed with PBS and nuclei were stained with Hoechst. After a final washing in PBS, slides were mounted with Fluoromount (Sigma-Aldrich). Microscopy analysis was performed using a Cell Observer SD-ApoTome laser scanning system (Carl Zeiss).

Quantitative Reverse Transcription Polymerase Chain Reaction

Mouse hepatic tissue was suspended in 1 ml of TRIzol™ solution (Ambion,Thermofisher) and homogenized in a Bullet blender (Next Advance Inc., New York, NY, USA) at a speed of 8 rpm for 3 min using 0.5 mm size zirconium beads. The homogenized tissue was collected and centrifuged at 12,000 g for 15 min at 4°C, and the supernatant from homogenized tissue was transferred to clean tubes and subjected to RNA according to manufacturer's protocol. Isolated RNA was quantified spectrophotometrically using NanoDrop 2000 (ThermoFisher Scientific). High-capacity cDNA reverse transcription Kit (Applied Biosystems™) was used to synthesize the cDNA from 200 ng of RNA. Then, a real-time polymerase chain reaction (RT-PCR) (Applied Biosystems™) was performed on duplicate cDNA samples according to the chemistry of Power SYBR® Green PCR Master Mix (Applied Biosystems™), using the primers described in supplementary material 2. Comparative ΔΔCt method was used to calculate the relative expression levels of the genes of interest normalized to the house-keeping gene expression Actinβ. Samples from the experimental sham group were used as reference for the quantitative analysis.

Statistical Analysis

Data are expressed as mean ± standard error of the mean (SEM). Statistical analyses were performed using one-way ANOVA with Newman-Keuls multiple comparison test where appropriate (GraphPad Prism, version 6.00, USA). A p value <0.05 was considered as statistically significant.

Results

Characterization of HLSC-EV

Figure 1a reports the NanoSight profile of purified HLSC-EV. The expression of HLSC- EV markers was performed using the multiplex bead-based flow cytometry assay platform for EV as previously described [24, 25]. HLSC-EV expressed CD9, CD63, and CD81 as well as high fluorescence intensity for CD29, CD44, CD105 and CD49e. At low-positive fluorescence intensity were also detected other markers such as CD142, CD146, SSEA-4, and MCSP (Fig. 1b). Hematopoietic (CD3, CD4, CD8, CD19, etc.), endothelial (CD31), and epithelial (CD326) markers were negative in HLSC-EV. Moreover, HLSC-EV showed a homogeneous pattern of nano-sized membrane vesicles as seen by transmission electron microscopy (Fig. 1c).

HLSC-EV Biodistribution

The fluorescence from dissected organs was quantified immediately with IVIS (Fig. 2a). In all study groups, the fluorescent signal was significantly higher in the liver compared to other organs (Fig. 2b). The biodistribution analysis demonstrated that Dil-Did stained HLSC-EV were mostly localized in the liver but a modest signal was also detected in the kidneys, intestine, pancreas, spleen, heart and lungs. In fact, the hepatic fluorescence in the treated groups was significantly higher than the hepatic fluorescence in the control group, that received saline solution alone, and in the sham operated group (all p values <0.0001) (Fig. 2b). Finally, the livers of animals treated with the EV1 dose were significantly more fluorescent than the livers of mice treated with the EV2 dose ($p < 0.05$) (Fig. 2b). A relative increase, even if not significant, in the IVIS signal was also observed in kidneys of mice treated with the EV2 (Figs. 2a and b).

Furthermore, the presence of Dil-Did stained HLSC-EV was revealed by immunofluorescence analysis. In particular,

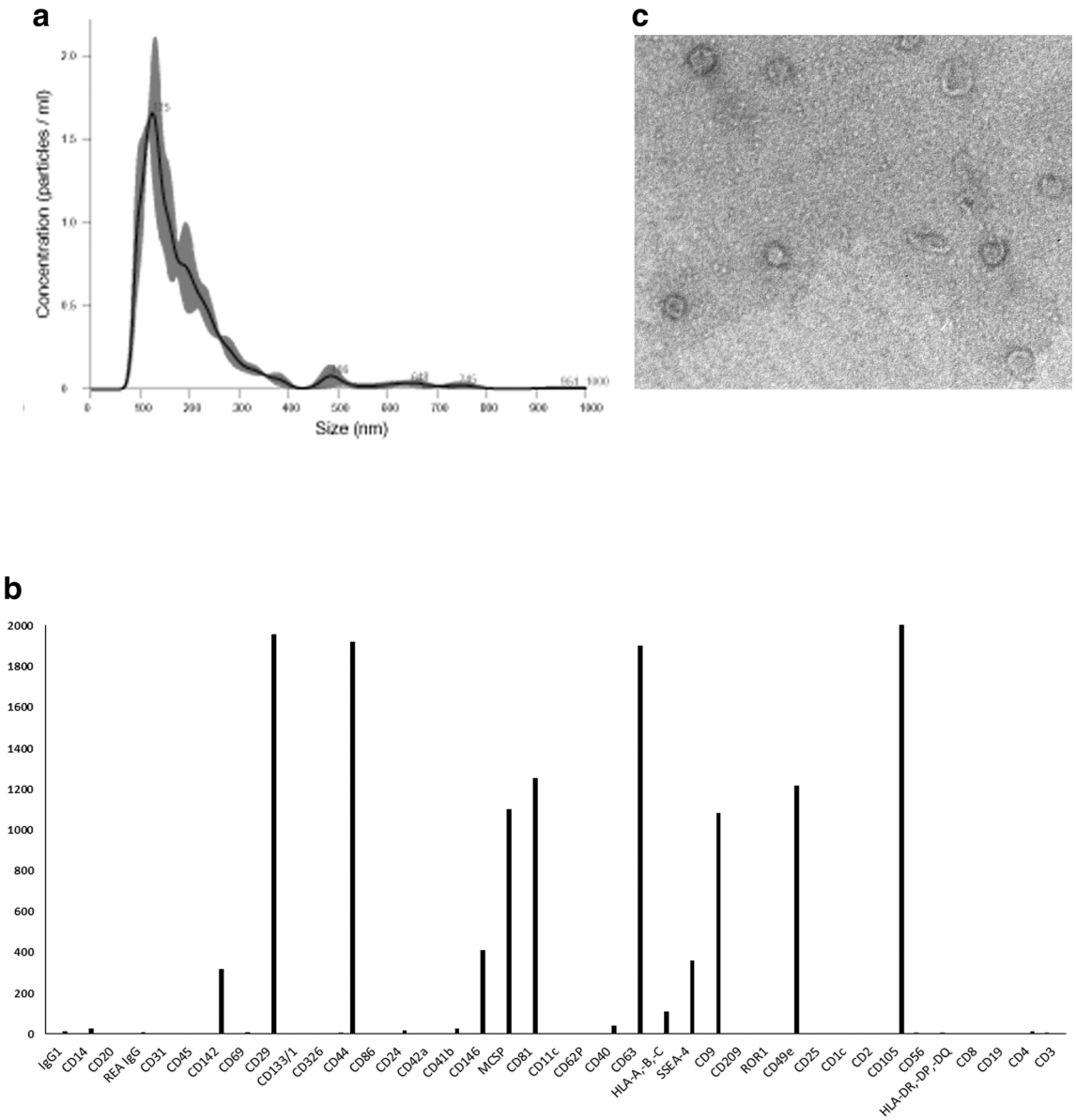

Fig. 1 Characterization of HLSC-EV. (**a**) Nanoparticle tracking analyses showing the size distribution of purified HLSC-EV. (**b**) Cytofluorimetric characterization of HLSC-EV by multiplex bead-based flow cytometry assay: 39 multiplexed populations of dye-labeled antibody-coated capture beads are incubated with HLSC-EV samples. Captured HLSC-EV were counterstained with pan tetraspanins APC-labeled detection antibodies. The graph shows a quantification of the median APC fluorescence values for all bead populations after background correction (medium control values subtracted from measured HLSC-EV values) of a representative HLSC-EV preparation. (**c**) Representative micrograph of transmission electron microscopy of HLSC-EV. EV negatively stained with NanoVan (scale bars = 100 nm, magnification ×100,000)

the HLSC-EV were able to integrate within the hepatocytes, as confirmed by colocalization with the cytokeratin-8 antibody, used as a hepatocyte marker (Fig. 2c).

Histological Analysis

Compared with sham livers, large areas of vascular congestion, cell vacuolization and hydropic degeneration were observed in IRI mice (Fig. 3a). The Suzuki's score quantification showed that the EV1 dose was able to reduce tissue damage, whereas this protective effect was not observed in the livers from the EV2 group, that were equal to controls. Since the animals were sacrificed after 6 h from IRI, hydropic degeneration was considered as a precursor of tissue necrosis that occurs in a longer period of time. In particular, the hydropic degeneration was significantly reduced in the EV1 group compared to control and EV2 group (EV1: 1.8 ± 0.37, control: 2.8 ± 0.17, EV2: 3.33 ± 0.17; $p < 0.05$), whereas vascular congestion and cell vacuolization were not modified (Fig. 3b). By contrast, livers from mice treated with the EV2 dose showed

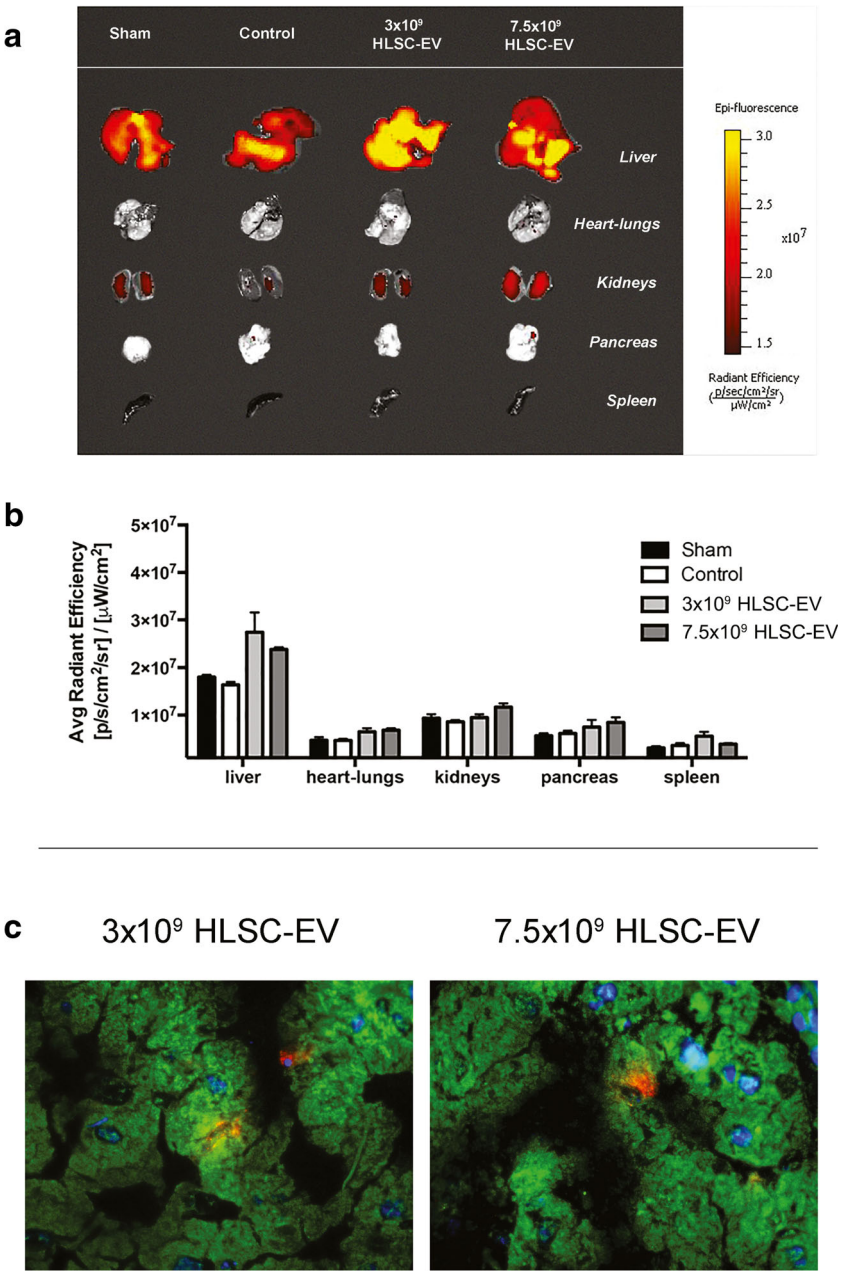

Fig. 2 Biodistribution and immunofluorescence of Dil/Did-stained HLSC-EV. (**a**) Liver, heart and lungs, kidneys, pancreas and spleen accumulation of Dil/Did-stained HLSC-EV. Livers from control and sham operated animals exhibit increased fluorescence compared to other organs due to the characteristic strong background fluorescent signal of the liver. (**b**) Intensity of fluorescent signal detected ex-vivo after 6 h. In all groups, liver vs other organs ($p < 0.0001$), EV1 liver vs control liver ($p < 0.0001$) and EV1 liver vs EV2 liver ($p < 0.01$). Data are represented as mean ± SEM. (**c**) Representative micrographs showing DAPI-stained cell nuclei (blue), mouse anti-human cytokeratin-8 antibody immunofluorescence (green) and Dil/Did-stained HLSC-EV (red) (original magnification 630×)

an increase in vascular congestion compared with those from sham mice (EV2: 1.78 ± 0.29, sham: 0.61 ± 0.14; $p < 0.05$) (Figs. 3a and b).

Biochemistry Analysis

Six hours after reperfusion, serum levels of AST (control: 923 ± 210, sham: 343 ± 66.7 UI/L), ALT (control: 1733 ± 233, sham: 79.3 ± 10.6 UI/L) and LDH (control: 15414 ± 1552, sham: 3026 ± 443 UI/L) were significantly increased in the control group compared to the sham group ($p < 0.01$) (Figs. 4a, b and c). ALT and LDH levels were reduced in EV1 group compared to the control group (ALT EV1: 524 ± 168, control: 1733 ± 233 UI/L; LDH EV1 7905 ± 1374, control: 15414 ± 1552 UI/L; all p values<0.01), whereas this reduction was not observed for the EV2 group, that did not differ from controls (Figs. 4b and c).

Molecular Biology

To investigate at a molecular level whether HLSC-EV ameliorate injured IRI livers, gene expression of factors involved in cellular damage pathways were analyzed by RT-PCR. The mRNA levels of inflammatory molecules such as tumor necrosis factor alpha (TNF-α), CXC motif chemokine 10 (CXCL-10), CC motif chemokine ligand 2 (CCL-2) and interleukin 10

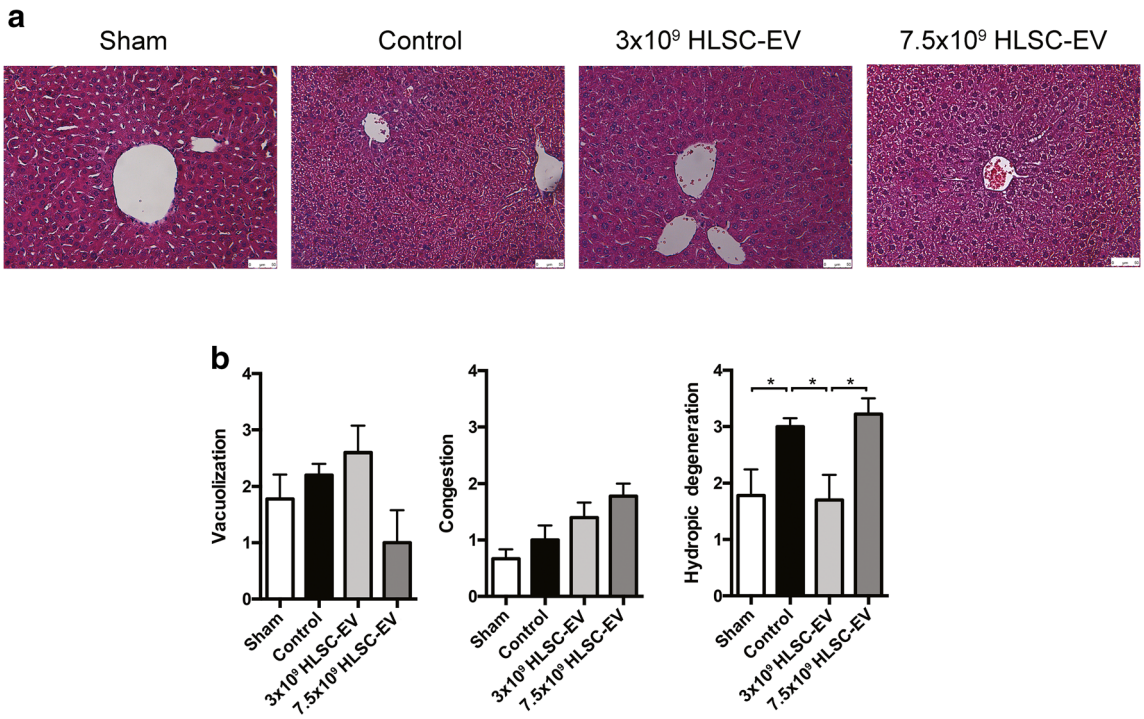

Fig. 3 Histological analysis showing the hepatoprotective activity of HLSC-EV against liver IRI. (**a**) Representative micrographs of H&E stain of liver tissues (original magnification 200×, scale bar 50 μm). (**b**) Quantitative scoring for tissue damage according to Suzuki's histological criteria (*$p < 0.05$). Data are represented as mean ± SEM

(IL-10) were increased at 6 h after the IRI induction ($p < 0.01$) (Figs. 5a-c, f). Compared to controls, expression levels of these mRNA were significantly reduced in HLSC-EV-treated IRI mice ($p < 0.05$), independently of the used dose (Figs. 5a, b, c). Expression of toll-like receptor 4 (TLR-4) and interleukin 6 (IL-6) mRNA were not affected by IRI and were not modulated by HLSC-EV treatment (Figs. 5d and e). Mean IL-6 mRNA level was higher in EV1 group, but this finding did not reach statistical significance (Fig. 5e).

We also evaluated mRNA expression of BCL-2-associated X protein (BAX) (pro-apoptotic; supplementary material 3A), B cell lymphoma 2 (BCL-2) (anti-apoptotic; supplementary material 3B), heme oxygenase 1 (HO-1) and sirtuin 1 (SIRT1) proteins (anti-oxidant and cytoprotective molecules; supplementary material 4A and B), hypoxia-inducible factor-1α (HIF-1α; supplementary material 5A), metalloproteinase inhibitor 1 precursor (TIMP1) and transforming growth factor-β1 (TGF-β1) proteins (pro-fibrotic; supplementary material 5B and C). RT-PCR analysis showed that only HO-1 mRNA levels exhibit a trend of increment in the IRI livers (supplementary material 4A), whereas TGF-β1 mRNA level (supplementary material 5C) was reduced in IRI group ($p < 0.01$). No modifications were observed in other analyzed mRNA (supplementary material 3A-B, 4B and 5A-C).

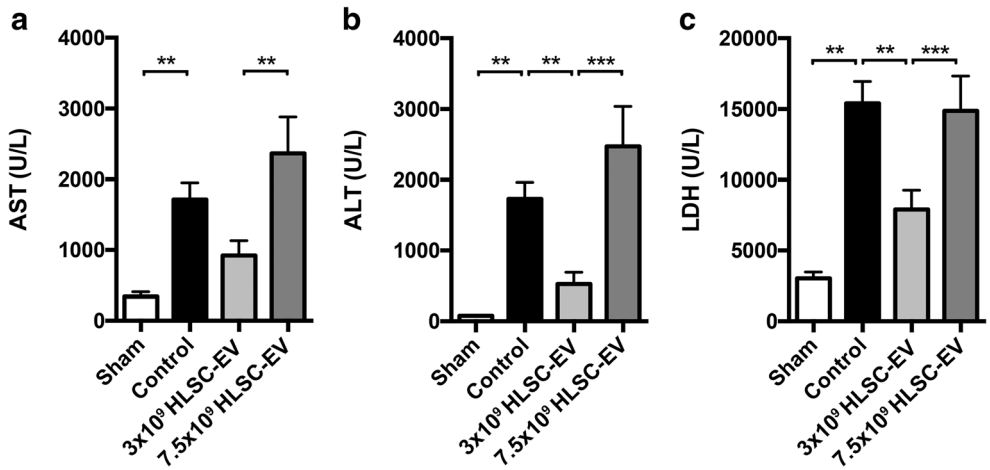

Fig. 4 Biochemical markers of liver injury showing the hepatoprotective activity of HLSC-EV against liver IRI. (**a**) Aspartate aminotransferase (**p < 0.01) (**b**) Alanine aminotransferase (**p < 0.01, ***$p < 0.001$) and (**c**) Lactate dehydrogenase (**p < 0.01, ***p < 0.001). Data are represented as mean ± SEM

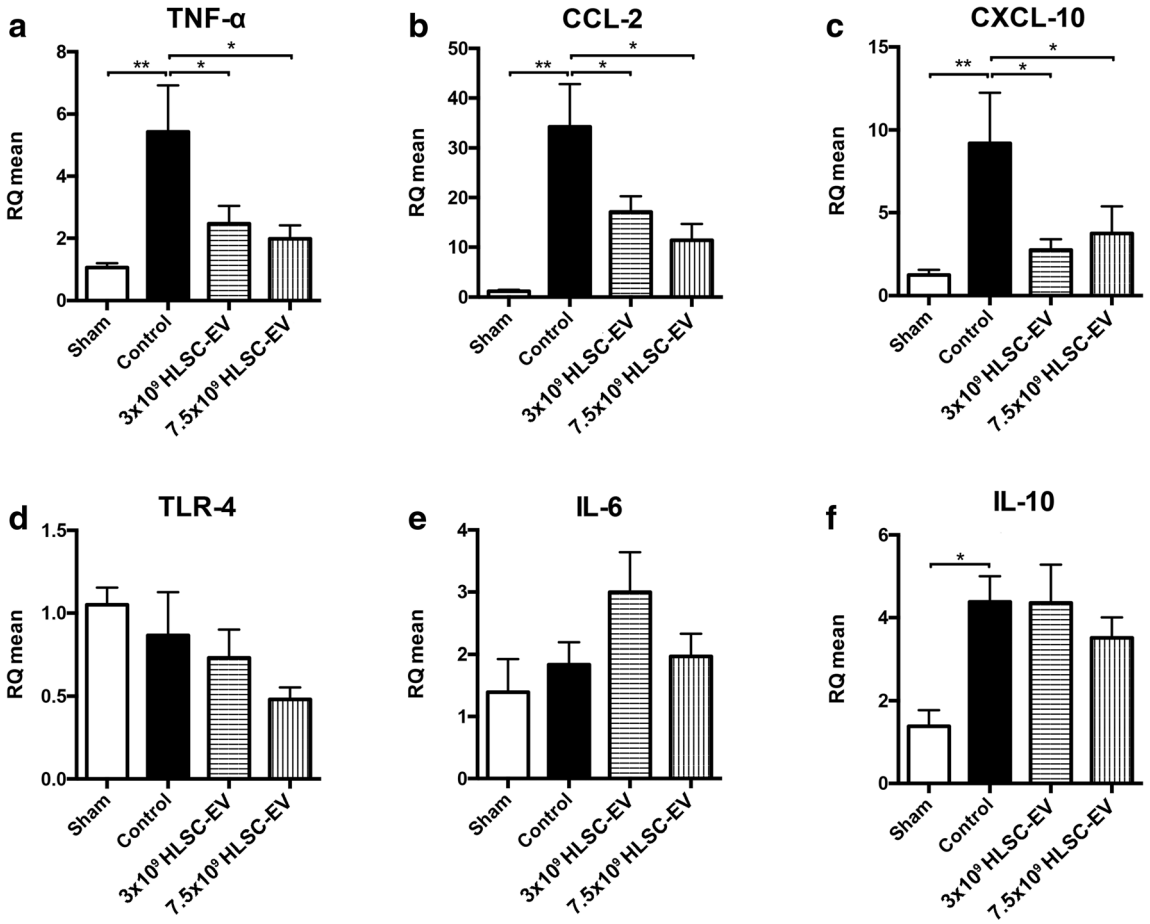

Fig. 5 Quantitative analysis of Real Time PCR on a selection of mouse genes involved in inflammation pathway. Mean relative quantification of RT-PCR analysis of (**a**) TNF-α, (**b**) CCL-2, (**c**) CXCL-10, (**d**) TLR-4, (**e**) IL-6, and (**f**) IL-10. (*$p < 0.05$, **$p < 0.01$). All values are normalized to Actin β. Data are represented as mean ± SEM

Discussion

Hepatic IRI can be observed in different clinical settings such as liver resection and liver transplantation. The severity of IRI is proportional to the duration of the ischemic phase, which is characterized by anaerobic metabolism, accumulation of lactates and acidification of the extracellular milieu [2, 28, 29]. The restoration of oxygen and nutrients supply at reperfusion determines a sudden increase of ROS production, leading to mitochondria and cell damage, and subsequent activation of neutrophils and Kupffer cells [1, 30–34], which in turn release pro-inflammatory chemokines and cytokines [35–39]. Consequently, hepatocytes death can occur by apoptosis and oncotic necrosis [40, 41].

With regard to the liver setting, HLSC-EV successfully promoted liver regeneration in a model of 70% hepatectomy in rats [20]. Moreover, we recently demonstrated that HLSC-EV were able to reduce liver injury in a model of hypoxic normothermic machine perfusion. In this setting, we observed that HLSC-EV treatment significantly decreased AST and LDH release in the perfusate, necrosis and apoptosis severity and HIF-1α and TGF-β1 expression [21]. Recently, in a mouse model of NASH, HLSC-EV-treated animals exhibited reduced fibrosis and inflammation and proteins carried by HLSC-EV were identified as possible mediators of these effects [19].

HLSC-EV can be stored for up to 6 months at −80°C without losing their biological activity, which represents a relevant advantage of their use over that of stem cells.

On this basis, our study aimed at evaluating the ability of HLSC-EV to protect the liver against warm IRI in an in vivo mouse model. For this purpose, we used a well described mouse model of hepatic IRI [42]. The duration of the ischemic phase was set at 90 min, as this is the reported limit for hepatocyte survival in murine models [43]. Immediately after clamp removal, HLSC-EV treatment was administered systemically by the tail vein. The two doses studied were defined according to our laboratory experience on the use of HLSC-EV in vivo, [8, 19, 44] and other authors' studies. All the animals were comparable in size and weight, resulting in low variability between the groups during surgical procedures. The biodistribution study confirmed the ability of HLSC-EV

to localize within the hepatocytes of the damaged liver [21]. IVIS analysis showed that hepatic fluorescence was higher than that of other organs in all treatment groups including the sham operated group suggesting that liver is the organ mainly involved in the clearance of EV from circulation. However, signal from the EV1 livers was significantly higher than the sham, control and EV2 livers, suggesting that in this group HLSC-EV were effectively integrated in the hepatic parenchyma. The reason for the lower liver localization of the higher dose of EV is unclear but correlate with the reduced protective effect of EV2 on IRI.

The release of cytolytic enzymes is widely considered as an important marker of liver injury in mouse models of hepatic IRI [42, 45–47]. The EV1 dose significantly reduced serum ALT and LDH when compared to the control group. Furthermore, EV1 group did not differ from the sham group in terms of ALT release, showing that HLSC-EV treatment strongly protected the hepatocytes from the ischemic insult. On the other hand, there was no difference in ALT and LDH levels between EV2 and control group, suggesting that a higher EV dose failed to protect the liver against IRI.

Histological analyses were consistent with biochemistry results. In particular, only EV1 dose was able to reduce the amount of hydropic degeneration as compared to the control group, confirming the role of the lower dose of HLSC-EV in limiting IRI [21]. These results suggest that when EV are administered at higher concentrations they lose the majority of their beneficial role. This unexpected effect may be explained by the lower hepatic concentration reached by the EV2 dose, or because at this higher dose they exert a procoagulant activity, that was demonstrated also by other researchers [48]. On the other hand, excluding the liver and a tendency in the kidneys, there were no differences in biodistribution between the two doses and no intrahepatic clotting was observed within the livers in our model. Thus, this aspect remains unclear and further investigations are warranted to better define this dose-response relationship.

In our study, HLSC-EV treatment resulted in a significant decrease of TNF-α, CCL-2 and CXCL-10 mRNA levels, which are key inflammatory molecules that participate in the post-reperfusion phase of IRI [35, 36, 38, 39]. The expression of TLR-4, IL-6 and IL-10 was not affected by HLSC-EV. Also, we noted that HO-1 and SIRT1 mRNA levels in the IRI group were not different from those observed in sham animals, suggesting the absence of oxidative damage at 6 h after reperfusion.

In this in vivo model, HLSC-EV treatment did not influence BAX and BCL-2 mRNA levels in the livers exposed to IRI, indicating a lack of modulating effects on apoptosis by HLSC-EV. Nevertheless, in EV1 group we observed a reduction in the degree of hydropic degeneration, a precursor of necrosis, which could therefore represent the main process involved in hepatocytes loss in our model [49]. Finally, hypoxia did not lead to an early activation of fibrosis pathways in our experiments, as HIF1-α and TGF-β1 mRNA levels were similar between sham and ischemic groups. Moreover, we observed that TIMP1, which is activated downstream in the fibrotic process initiated by TGF-β1, was not activated, due to the lack of TGF-β1 activation.

Overall, our data suggest that the HLSC-EV are able reduce liver IRI by modulating the inflammatory status which characterizes the early phases of IRI, by acting at the beginning of the inflammatory cascade. Indeed, TNF-α is involved in the activation of chemokines cascade and it is produced by activated macrophages, $CD4^+$ lymphocytes, neutrophils, mast cells and eosinophils, whereas CXCL-10 and CCL-2 are mainly secreted by Kupffer cells during hepatic inflammation, promoting neutrophils attraction [50, 51]. In our study, HLSC-EV reduced the production of TNF-α and, as a consequence, the production of the two other chemokines CXCL-10 and CCL-2, which are located downstream in the activation of the inflammatory cascade, thus ameliorating the local inflammation induced by the ischemia-reperfusion damage. Interestingly, also the EV2 dose was able to reduce the expression of TNF-α, CCL-2 and CXCL-10 genes, but this beneficial effect was observed only at molecular level and was not supported by biochemistry and histology results.

We observed that, after six hours of reperfusion, some key genes involved in inflammation were upregulated by IRI, and some of these genes were also modulated by HLSC-EV. This beneficial effect was also demonstrated by the reduction of cytolysis markers and hydropic degeneration in the animals treated with the lower dose of HLSC-EV. However, we acknowledge that our preliminary study presents certain limitations. In particular, we focused our attention on the acute phase of liver IRI and long-term effects were not investigated at this time. Since in our previous experience we found that HLSC-EV exert their properties within the first hours from reperfusion, our intention was to better understand the biological and molecular mechanisms involved in their early activity. It would be interesting in future studies to evaluate harder clinical outcomes, such as longer follow-up times and survival analyses.

In conclusion, this study demonstrates that a dose of 3×10^9 HLSC-EV was able to protect the liver from IRI, whereas a dose of 7.5×10^9 HLSC-EV was ineffective in ameliorating liver function, with only an anti-inflammatory modulation effect observed only at molecular level.

Altogether, these data may suggest that systemic administration of HLSC-EV could be considered as an alternative cell-based approach for hepatic ischemia reperfusion injury. Nevertheless, additional investigations are needed to further support the potential use of HLSC-EV in clinical settings.

Supplementary Information The online version contains supplementary material available at https://doi.org/10.1007/s12015-020-10078-7.

Acknowledgments We thank Unicyte for the fruitful discussions and guidance on their proprietary HLSC technology which was used in this research project. Authors would like to thank Roberta Moscuzza, Giulia Felisio, Aurora Schiavon, Matteo Curcio and Francesca Sivieri for their technical assistance.

Author Contributions A.C. and D. R. contributed equally to this work. Experimental procedures, data collection and analysis were performed by A.C., D.R., V.N.T., N.D.S., C.P., G.F. and F.R.; E.D., F.A. and P.C. contributed in histopathological and biochemistry analyses; D.P., S.B. and R.R. designed the study, analyzed the data and revised the article. All authors read and approved the final version of the manuscript.

Funding Open access funding provided by Università degli Studi di Torino within the CRUI-CARE Agreement.. This study was funded by Ricerca Locale Ex 60%, University of Turin - Years 2015 and Year 2016.

Compliance with Ethical Standards

Conflict of Interest All authors declare that they have no competing interests.

References

1. Chouchani, E. T., Pell, V. R., James, A. M., Work, L. M., Saeb-Parsy, K., Frezza, C., Krieg, T., & Murphy, M. P. (2016). A unifying mechanism for mitochondrial superoxide production during ischemia-reperfusion injury. *Cell Metabolism, 23*(2), 254–263. https://doi.org/10.1016/j.cmet.2015.12.009.
2. Zhai, Y., Petrowsky, H., Hong, J. C., Busuttil, R. W., & Kupiec-Weglinski, J. W. (2013). Ischaemia-reperfusion injury in liver transplantation-from bench to bedside. *Nature Reviews Gastroenterology and Hepatology, 10*(2), 79–89. https://doi.org/10.1038/nrgastro.2012.225.
3. Konishi, T., & Lentsch, A. B. (2017). Hepatic ischemia/reperfusion: Mechanisms of tissue injury, repair, and regeneration. *Gene Expression, 17*(4), 277–287. https://doi.org/10.3727/105221617X15042750874156.
4. Peralta, C., Jiménez-Castro, M. B., & Gracia-Sancho, J. (2013). Hepatic ischemia and reperfusion injury: Effects on the liver sinusoidal milieu. *Journal of Hepatology, 59*(5), 1094–1106. https://doi.org/10.1016/j.jhep.2013.06.017.
5. Farmer, D. G., Amersi, F., Kupiec-Weglinski, J., & Busuttil, R. W. (2000). Current status of ischemia and reperfusion injury in the liver. *Transplantation Reviews, 14*(2), 106–126. https://doi.org/10.1053/tr.2000.4651.
6. Herrera, M. B., Bruno, S., Buttiglieri, S., Tetta, C., Gatti, S., Deregibus, M. C., Bussolati, B., & Camussi, G. (2006). Isolation and characterization of a stem cell population from adult human liver. *Stem Cells, 24*(12), 2840–2850. https://doi.org/10.1634/stemcells.2006-0114.
7. Herrera, M. B., Fonsato, V., Bruno, S., Grange, C., Gilbo, N., Romagnoli, R., Tetta, C., & Camussi, G. (2013). Human liver stem cells improve liver injury in a model of fulminant liver failure. *Hepatology, 57*(1), 311–319. https://doi.org/10.1002/hep.25986.
8. Herrera, M. B., Bruno, S., Grange, C., Tapparo, M., Cantaluppi, V., Tetta, C., & Camussi, G. (2014). Human liver stem cells and derived extracellular vesicles improve recovery in a murine model of acute kidney injury. *Stem Cell Research and Therapy, 5*(6), 124. https://doi.org/10.1186/scrt514.
9. Navarro-Tableros, V., Herrera Sanchez, M. B., Figliolini, F., Romagnoli, R., Tetta, C., & Camussi, G. (2015). Recellularization of rat liver scaffolds by human liver stem cells. *Tissue Engineering Part A, 21*(11–12), 1929–1939. https://doi.org/10.1089/ten.tea.2014.0573.
10. Spada, M., Porta, F., Righi, D., Gazzera, C., Tandoi, F., Ferrero, I., Fagioli, F., Sanchez, M. B. H., Calvo, P. L., Biamino, E., Bruno, S., Gunetti, M., Contursi, C., Lauritano, C., Conio, A., Amoroso, A., Salizzoni, M., Silengo, L., Camussi, G., & Romagnoli, R. (2020). Intrahepatic Administration of Human Liver Stem Cells in infants with inherited neonatal-onset Hyperammonemia: A phase I study. *Stem Cell Reviews and Reports, 16*(1), 186–197. https://doi.org/10.1007/s12015-019-09925-z.
11. Camussi, G., Deregibus, M. C., & Cantaluppi, V. (2013). Role of stem-cell-derived microvesicles in the paracrine action of stem cells. *Biochemical Society Transactions, 41*(1), 283–287. https://doi.org/10.1042/bst20120192.
12. Lo Cicero, A., Stahl, P. D., & Raposo, G. (2015). Extracellular vesicles shuffling intercellular messages: For good or for bad. *Current Opinion in Cell Biology, 35*, 69–77. https://doi.org/10.1016/j.ceb.2015.04.013.
13. van Niel, G., D'Angelo, G., & Raposo, G. (2018). Shedding light on the cell biology of extracellular vesicles. *Nature Reviews. Molecular Cell Biology, 19*(4), 213–228. https://doi.org/10.1038/nrm.2017.125.
14. Maas, S. L. N., Breakefield, X. O., & Weaver, A. M. (2017). Extracellular vesicles: Unique intercellular delivery vehicles. *Trends in Cell Biology, 27*(3), 172–188. https://doi.org/10.1016/j.tcb.2016.11.003.
15. Mathieu, M., Martin-Jaular, L., Lavieu, G., & Théry, C. (2019). Specificities of secretion and uptake of exosomes and other extracellular vesicles for cell-to-cell communication. *Nature Cell Biology, 21*(1), 9–17. https://doi.org/10.1038/s41556-018-0250-9.
16. Record, M., Carayon, K., Poirot, M., & Silvente-Poirot, S. (2014). Exosomes as new vesicular lipid transporters involved in cell-cell communication and various pathophysiologies. *Biochimica et Biophysica Acta - Molecular and Cell Biology of Lipids, 1841*(1), 108–120. https://doi.org/10.1016/j.bbalip.2013.10.004.
17. Quesenberry, P. J., Aliotta, J., Deregibus, M. C., & Camussi, G. (2015). Role of extracellular RNA-carrying vesicles in cell differentiation and reprogramming. *Stem Cell Research and Therapy, 6*(1), 1–10. https://doi.org/10.1186/s13287-015-0150-x.
18. Baghaei, K., Tokhanbigli, S., Asadzadeh, H., Nmaki, S., Reza Zali, M., & Hashemi, S. M. (2019). Exosomes as a novel cell-free therapeutic approach in gastrointestinal diseases. *Journal of Cellular Physiology, 234*(7), 9910–9926. https://doi.org/10.1002/jcp.27934.
19. Bruno, S., Pasquino, C., Herrera Sanchez, M. B., Tapparo, M., Figliolini, F., Grange, C., Chiabotto, G., Cedrino, M., Deregibus, M. C., Tetta, C., & Camussi, G. (2020). HLSC-derived extracellular vesicles attenuate liver fibrosis and inflammation in a murine model of non-alcoholic Steatohepatitis. *Molecular Therapy, 28*(2), 479–489. https://doi.org/10.1016/j.ymthe.2019.10.016.
20. Herrera, M. B., Fonsato, V., Gatti, S., Deregibus, M. C., Sordi, A., Cantarella, D., Calogero, R., Bussolati, B., Tetta, C., & Camussi, G.

(2010). Human liver stem cell-derived microvesicles accelerate hepatic regeneration in hepatectomized rats. *Journal of Cellular and Molecular Medicine, 14*(6 B), 1605–1618. https://doi.org/10.1111/j.1582-4934.2009.00860.x.

21. Rigo, F., De Stefano, N., Navarro-Tableros, V., David, E., Rizza, G., Catalano, G., Gilbo, N., Maione, F., Gonella, F., Roggio, D., Martini, S., Patrono, D., Mauro, S., Camussi, G., & Romagnoli, R. (2018). Extracellular vesicles from human liver stem cells reduce injury in an ex vivo Normothermic hypoxic rat liver perfusion model. *Transplantation, 102*(5), e205–e210. https://doi.org/10.1097/tp.0000000000002123.
22. Grange, C., Tapparo, M., Bruno, S., Chatterjee, D., Quesenberry, P. J., Tetta, C., & Camussi, G. (2014). Biodistribution of mesenchymal stem cell-derived extracellular vesicles in a model of acute kidney injury monitored by optical imaging. *International Journal of Molecular Medicine, 33*(5), 1055–1063. https://doi.org/10.3892/ijmm.2014.1663.
23. Bruno, S., Grange, C., Collino, F., Deregibus, M. C., Cantaluppi, V., Biancone, L., Tetta, C., & Camussi, G. (2012). Microvesicles derived from mesenchymal stem cells enhance survival in a lethal model of acute kidney injury. *PLoS One, 7*(3), e33115. https://doi.org/10.1371/journal.pone.0033115.
24. Koliha, N., Wiencek, Y., Heider, U., Jüngst, C., Kladt, N., Krauthäuser, S., Johnston, I. C. D., Bosio, A., Schauss, A., & Wild, S. (2016). A novel multiplex bead-based platform highlights the diversity of extracellular vesicles. *Journal of Extracellular Vesicles, 5*, 29975. https://doi.org/10.3402/jev.v5.29975.
25. Wiklander, O. P. B., Bostancioglu, R. B., Welsh, J. A., Zickler, A. M., Murke, F., Corso, G., Felldin, U., Hagey, D. W., Evertsson, B., Liang, X. M., Gustafsson, M. O., Mohammad, D. K., Wiek, C., Hanenberg, H., Bremer, M., Gupta, D., Björnstedt, M., Giebel, B., Nordin, J. Z., Jones, J. C., el Andaloussi, S., & Görgens, A. (2018). Systematic methodological evaluation of a multiplex bead-based flow cytometry assay for detection of extracellular vesicle surface signatures. *Frontiers in Immunology, 9*, 1326. https://doi.org/10.3389/fimmu.2018.01326.
26. Deregibus, M. C., Figliolini, F., D'Antico, S., Manzini, P. M., Pasquino, C., De Lena, M., Tetta, C., Brizzi, M. F., & Camussi, G. (2016). Charge-based precipitation of extracellular vesicles. *International Journal of Molecular Medicine, 38*(5), 1359–1366. https://doi.org/10.3892/ijmm.2016.2759.
27. Suzuki, S., Toledo-Pereyra, L. H., Rodriguez, F. J., & Cejalvo, D. (1993). Neutrophil infiltration as an important factor in liver ischemia and reperfusion injury: Modulating effects of FK506 and cyclosporine. *Transplantation, 55*(6), 1265–1272. https://doi.org/10.1097/00007890-199306000-00011.
28. Cannistrà, M., Ruggiero, M., Zullo, A., Gallelli, G., Serafini, S., Maria, M., Naso, A., Grande, R., Serra, R., & Nardo, B. (2016). Hepatic ischemia reperfusion injury: A systematic review of literature and the role of current drugs and biomarkers. *International Journal of Surgery, 33*, S57–S70. https://doi.org/10.1016/j.ijsu.2016.05.050.
29. Eltzschig, H. K., & Eckle, T. (2011). Ischemia and reperfusion-from mechanism to translation. *Nature Medicine, 17*(11), 1391–1401. https://doi.org/10.1038/nm.2507.
30. Quesnelle, K. M., Bystrom, P. V., & Toledo-Pereyra, L. H. (2015). Molecular responses to ischemia and reperfusion in the liver. *Archives of Toxicology, 89*(5), 651–657. https://doi.org/10.1007/s00204-014-1437-x.
31. Jaeschke, H., Farhood, A., & Smith, C. W. (1990). Neutrophils contribute to ischemia/reperfusion injury in rat liver in vivo. *The FASEB Journal, 4*(15), 3355–3359. https://doi.org/10.1096/fasebj.4.15.2253850.
32. Li, P., He, K., Li, J., Liu, Z., & Gong, J. (2017). The role of Kupffer cells in hepatic diseases. *Molecular Immunology, 85*, 222–229. https://doi.org/10.1016/j.molimm.2017.02.018.
33. Wanner, G. A., Ertel, W., Müller, P., Höfer, Y., Leiderer, R., Menger, M. D., & Messmer, K. (1996). Liver ischemia and reperfusion induces a systemic inflammatory response through Kupffer cell activation. *Shock, 5*(1), 34–40. https://doi.org/10.1097/00024382-199601000-00008.
34. Caban, A., Oczkowicz, G., Abdel-Samad, O., & Cierpka, L. (2002). Influence of Kupffer cells on the early phase of liver reperfusion. *Transplantation Proceedings, 34*(2), 694–697. https://doi.org/10.1016/S0041-1345(01)02891-3.
35. van Golen, R. F., van Gulik, T. M., & Heger, M. (2012). The sterile immune response during hepatic ischemia/reperfusion. *Cytokine and Growth Factor Reviews, 23*(3), 69–84. https://doi.org/10.1016/j.cytogfr.2012.04.006.
36. Colletti, L. M., Remick, D. G., Burtch, G. D., Kunkel, S. L., Strieter, R. M., & Campbell, D. A. (1990). Role of tumor necrosis factor-a in the pathophysiologic alterations after hepatic ischemia/reperfusion injury in the rat. *Journal of Clinical Investigation, 85*(6), 1936–1943.
37. Camargo, C. A., Madden, J. F., Gao, W., Selvan, R. S., & Clavien, P. A. (1997). Interleukin-6 protects liver against warm ischemia/reperfusion injury and promotes hepatocyte proliferation in the rodent. *Hepatology, 26*(6), 1513–1520. https://doi.org/10.1002/hep.510260619.
38. Zhang, J., Xu, P., Song, P., Wang, H., Zhang, Y., Hu, Q., Wang, G., Zhang, S., Yu, Q., Billiar, T. R., Wang, C., & Zhang, J. (2016). CCL2-CCR2 signaling promotes hepatic ischemia/reperfusion injury. *Journal of Surgical Research, 202*(2), 352–362. https://doi.org/10.1016/j.jss.2016.02.029.
39. Saiman, Y., & Friedman, S. L. (2012). The role of chemokines in acute liver injury. *Frontiers in Physiology, 3*, 213. https://doi.org/10.3389/fphys.2012.00213.
40. Jaeschke, H., & Lemasters, J. J. (2003). Apoptosis versus oncotic necrosis in hepatic ischemia/reperfusion injury. *Gastroenterology, 125*(4), 1246–1257. https://doi.org/10.1016/S0016-5085(03)01209-5.
41. Franchello, A., Gilbo, N., David, E., Ricchiuti, A., Romagnoli, R., Cerutti, E., & Salizzoni, M. (2009). Ischemic preconditioning (IP) of the liver as a safe and protective technique against ischemia/reperfusion injury (IRI). *American Journal of Transplantation, 9*(7), 1629–1639. https://doi.org/10.1111/j.1600-6143.2009.02680.x.
42. Abe, Y., Hines, I. N., Zibari, G., Pavlick, K., Gray, L., Kitagawa, Y., & Grisham, M. B. (2009). Mouse model of liver ischemia and reperfusion injury: Method for studying reactive oxygen and nitrogen metabolites in vivo. *Free Radical Biology and Medicine, 46*(1), 1–7. https://doi.org/10.1016/j.freeradbiomed.2008.09.029.
43. Gonzalez-Flecha, B., Cutrin, J. C., & Boveris, A. (1993). Time course and mechanism of oxidative stress and tissue damage in rat liver subjected to in vivo ischemia-reperfusion. *Journal of Clinical Investigation, 91*(2), 456–464. https://doi.org/10.1172/JCI116223.
44. Kholia, S., Herrera, M. B., Cedrino, M., Papadimitriou, E., Tapparo, M., Deregibus, M. C., Brizzi, M. F., Tetta, C., & Camussi, G. (2018). Human liver stem cell-derived extracellular vesicles prevent aristolochic acid-induced kidney fibrosis. *Frontiers in Immunology, 9*, 1639. https://doi.org/10.3389/fimmu.2018.01639.
45. Chouillard, E. K., Gumbs, A. A., & Cherqui, D. (2010). Vascular clamping in liver surgery: Physiology, indications and techniques. *Annals of Surgical Innovation and Research, 4*, 2. https://doi.org/10.1186/1750-1164-4-2.
46. Haga, H., Yan, I. K., Borrelli, D. A., Matsuda, A., Parasramka, M., Shukla, N., Lee, D. D., & Patel, T. (2017). Extracellular vesicles from bone marrow–derived mesenchymal stem cells protect against murine hepatic ischemia/reperfusion injury. *Liver Transplantation, 23*(6), 791–803. https://doi.org/10.1002/lt.24770.

47. Yao, J., Zheng, J., Cai, J., Zeng, K., Zhou, C., Zhang, J., Li, S., Li, H., Chen, L., He, L., Chen, H., Fu, H., Zhang, Q., Chen, G., Yang, Y., & Zhang, Y. (2019). Extracellular vesicles derived from human umbilical cord mesenchymal stem cells alleviate rat hepatic ischemia-reperfusion injury by suppressing oxidative stress and neutrophil inflammatory response. *FASEB Journal : Official Publication of the Federation of American Societies for Experimental Biology, 33*(2), 1695–1710. https://doi.org/10.1096/fj.201800131RR.
48. Silachev, D., Goryunov, K., Shpilyuk, M., Beznoschenko, O., Morozova, N., Kraevaya, E., Popkov, V., Pevzner, I., Zorova, L., Evtushenko, E., Starodubtseva, N., Kononikhin, A., Bugrova, A., Evtushenko, E., Plotnikov, E., Zorov, D., & Sukhikh, G. (2019). Effect of MSCs and MSC-derived extracellular vesicles on human blood coagulation. *Cells, 8*(3), 258. https://doi.org/10.3390/cells8030258.
49. Cursio, R., Colosetti, P., & Gugenheim, J. (2015). Autophagy and liver ischemia-reperfusion injury. *BioMed Research International, 2015*, 417590–417516. https://doi.org/10.1155/2015/417590.
50. Zhai, Y., Busuttil, R. W., & Kupiec-Weglinski, J. W. (2011). Liver ischemia and reperfusion injury: New insights into mechanisms of innate-adaptive immune-mediated tissue inflammation. *American Journal of Transplantation, 11*(8), 1563–1569. https://doi.org/10.1111/j.1600-6143.2011.03579.x.
51. Datta, G., Fuller, B. J., & Davidson, B. R. (2013). Molecular mechanisms of liver ischemia reperfusion injury: Insights from transgenic knockout models. *World Journal of Gastroenterology, 19*(11), 1683–1698. https://doi.org/10.3748/wjg.v19.i11.1683.

Affiliations

Alberto Calleri[1] · Dorotea Roggio[1] · Victor Navarro-Tableros[2] · Nicola De Stefano[1] · Chiara Pasquino[3] · Ezio David[4] · Giada Frigatti[1] · Federica Rigo[1] · Federica Antico[5] · Paola Caropreso[6] · Damiano Patrono[1] · Stefania Bruno[3] · Renato Romagnoli[1]

[1] General Surgery 2U, Liver Transplantation Center, AOU Città della Salute e della Scienza di Torino, University of Turin, Turin, Italy

[2] Scarl. - Molecular Biotechnology Center (MBC), 2i3T - Società per la gestione dell'incubatore di imprese e per il trasferimento tecnologico dell'Università degli Studi di Torino, Turin, Italy

[3] Department of Medical Sciences, University of Turin, Turin, Italy

[4] Pathology Unit, Molinette Hospital, AOU Città della Salute e della Scienza di Torino, Turin, Italy

[5] Forb – Fondazione per la Ricerca Biomedica, ONLUS - Molecular Biotechnology Center (MBC), Turin, Italy

[6] Clinical Biochemistry Laboratory, Molinette Hospital, AOU Città della Salute e della Scienza di Torino, Turin, Italy